

Journal Pre-proofs

Secretome of human adipose-derived mesenchymal stem cell relieves pain and neuroinflammation independently of the route of administration in experimental osteoarthritis

Giada Amodeo, Stefania Niada, Giorgia Moschetti, Silvia Franchi, Paolo Savadori, Anna T. Brini, Paola Sacerdote

PII: S0889-1591(21)00113-6
DOI: <https://doi.org/10.1016/j.bbi.2021.03.011>
Reference: YBRBI 4509

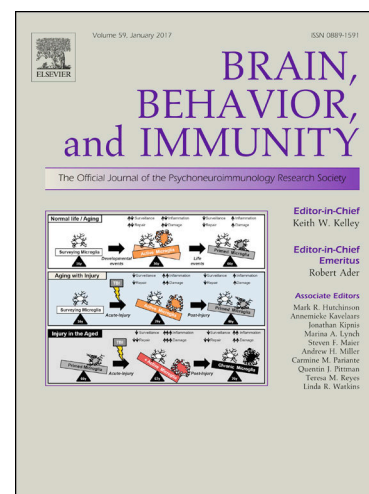
To appear in: *Brain, Behavior, and Immunity*

Received Date: 20 October 2020
Revised Date: 8 March 2021
Accepted Date: 11 March 2021

Please cite this article as: Amodeo, G., Niada, S., Moschetti, G., Franchi, S., Savadori, P., Brini, A.T., Sacerdote, P., Secretome of human adipose-derived mesenchymal stem cell relieves pain and neuroinflammation independently of the route of administration in experimental osteoarthritis, *Brain, Behavior, and Immunity* (2021), doi: <https://doi.org/10.1016/j.bbi.2021.03.011>

This is a PDF file of an article that has undergone enhancements after acceptance, such as the addition of a cover page and metadata, and formatting for readability, but it is not yet the definitive version of record. This version will undergo additional copyediting, typesetting and review before it is published in its final form, but we are providing this version to give early visibility of the article. Please note that, during the production process, errors may be discovered which could affect the content, and all legal disclaimers that apply to the journal pertain.

© 2021 Elsevier Inc. All rights reserved.



Secretome of human adipose-derived mesenchymal stem cell relieves pain and neuroinflammation independently of the route of administration in experimental osteoarthritis

Giada Amodeo PhD^a, Stefania Niada PhD^b, Giorgia Moschetti PhD^a, Silvia Franchi PhD^a, Paolo Savadori PhD^b, Anna T. Brini PhD^{b,c,#} Paola Sacerdote PhD^{a*#}

Anna T. Brini and Paola Sacerdote equally contributed to this work: co- last authors

^a Dipartimento di Scienze Farmacologiche e Biomolecolari, University of Milano, Milano, Italy

^b IRCCS Istituto Ortopedico Galeazzi, Milano, Italy

^c Dipartimento di Scienze Biomediche Chirurgiche e Odontoiatriche, University of Milano, Milano, Italy

* Corresponding author:

Paola Sacerdote

Dipartimento di Scienze Farmacologiche e Biomolecolari

Università degli studi di Milano

Via Vanvitelli 32

20129 Milano

Tel: 0250316929

paola.sacerdote@unimi.it

Declarations of interest : none

Running head: effect of hASC-secretome in OA pain

ABSTRACT

Objective: Treatment of pain associated with osteoarthritis (OA) is unsatisfactory and innovative approaches are needed. The secretome from human adipose-derived mesenchymal stem cells (hASC-Conditioned Medium, CM) has been successfully used to relieve painful symptoms in models of chronic pain. The aim of this study was to explore the efficacy of the hASC-CM to control pain and neuroinflammation in an animal model of OA.

Methods: OA was induced in mice by intra-articular monosodium-iodoacetate (MIA) injection. Thermal hyperalgesia and mechanical allodynia were assessed. Once hypersensitivity was established (7 days after MIA), hASC-CM was injected by IA, IPL and IV route and its effect monitored over time. Neuroinflammation in nerve, dorsal root ganglia and spinal cord was evaluated measuring proinflammatory markers and mediators by RT-qPCR. Protein content analysis of secretome by Mass Spectrometry was performed.

Results: A single injection with hASC-CM induced a fast and long lasting antihyperalgesic and antiallodynic effect. The IV route of administration appeared to be the most efficacious although all the treatments were effective. The effect on pain correlated with the ability of hASC-CM to reduce the neuroinflammatory condition in both the peripheral and central nervous system. Furthermore, the secretome analysis revealed 101 factors associated with immune regulation.

Conclusion: We suggest that hASC-CM is a valid treatment option for controlling OA-related hypersensitivity, exerting a rapid and long lasting pain relief. The mechanisms underpinning its effects are likely linked to the positive modulation of neuroinflammation in peripheral and central nervous system that sustains peripheral and central sensitization.

1. INTRODUCTION

Osteoarthritis (OA) is the most common form of chronic degenerative joint disease, affecting millions of people worldwide (Hunter et al., 2014; Mandl, 2019). It is characterized by the articular cartilage breakdown, subchondral bone remodeling, osteophyte formation and synovitis. It is suggested that both mechanical factors and inflammation cause a progressive joint damage (Barr et al., 2015; Felson et al., 2013). Although in patients there is a discrepancy between joint damage and painful manifestations, pain is a recurrent symptom in OA and the primary reason to seek medical help (Rainbow et al., 2012; Barr et al., 2015; Bedson and Croft, 2008). Current strategies for pain management are not satisfactory and often associated with substantial adverse effects (Alshami, 2014).

In the osteoarthritic joint, cells, such as synoviocytes, inflammatory cells, or chondrocytes produce chemokines, cytokines, and proteases, which can sensitize primary sensory neuron afferents (Orita et al., 2011; Schaible, 2012). The continuous increased nociceptive input from the periphery further results in central sensitization in dorsal horn spinal cord. Pathological changes in the joint cause hyperexcitability of the dorsal horn neurons (Grubb et al., 1993; Orita et al., 2011; Schaible, 2012), reducing their thresholds and enhancing their responses to knee stimulation. These sensitized dorsal horn neurons expand their receptive fields, a mechanism that underlies the spread of hypersensitivity from the knee joint to adjacent areas. The expansion of receptive fields and the reduction of mechanical thresholds around the joint area are consistently observed in OA patients (Arendt-Nielsen et al., 2010).

The development of neuroinflammation in dorsal root ganglia (DRG) and spinal cord has been described in rodent models of OA (Zhang et al., 2013; Haywood et al., 2018; de Sousa Valente, 2019). Neuroinflammation is characterized by microglia and astrocyte activation and by the production and release of proinflammatory cytokines and chemokines that sensitize neurons. Neuroinflammation is a common feature of different types of chronic pain (Thakur et al., 2012; Haywood et al., 2018). Indeed, some authors

have suggested that in OA a neuropathic pain component may be present (Thakur et al., 2012; Haywood et al., 2018). Interestingly, in experimental models, the modulation of neuroinflammation by different pharmacological treatments has been positive in relieving OA associated pain (de Sousa Valente, 2019).

In the search for novel effective treatments, stem cells and their secretome have been successfully applied to ameliorate pain in several conditions. More than 300 clinical trials have assessed/ are evaluating the safety and efficacy of Mesenchymal Stem Cells (MSCs) for pain management (clinicaltrials.gov;condition or disease: pain; other terms: MSC; Status: Active, not recruiting/ completed). MSCs were initially proposed in regenerative medicine based on their differentiation potential in several orthopedic conditions (Steinert et al., 2012; de Girolamo et al., 2015). However, the lack of a correlation between functional improvement and effective cell engraftment and/or differentiation *in situ* has led to the assumption that MSCs exert their effects primarily through their secreted products. Many studies provide pivotal support for this paracrine hypothesis and MSC-based therapy is increasingly focused on their secreted factors rather than their differentiation ability (Caplan, 2017; Crivelli et al., 2017). The MSC secretome, defined as the set of MSC-derived bioactive factors (soluble proteins, nucleic acids, lipids and extracellular vesicles), showed therapeutic effects similar to those observed after MSC transplantation (Harrell et al., 2019; Praveen Kumar et al., 2019), bypassing some drawbacks of cell-based therapy, such as undesired differentiation and potential activation of allogeneic immune response (Lukomska et al., 2019; Volarevic et al., 2018). Therapeutic effects of MSC secretome depend upon its ability to reach target cells and deliver genetic material, growth and immunomodulatory factors.

We previously demonstrated that intravenously injected human adipose-derived MSC (hASC) secretome was able to decrease neuropathic pain in diabetic mice, throughout a

modulation of peripheral immune responses and a reduction of the neuroinflammatory conditions in DRG and spinal cord (Brini et al., 2017).

The monosodium-iodoacetate (MIA)-induced OA model is largely used to evaluate pain and possible therapies in mice and rats. Intra-articular (IA) MIA injection results in functional impairment similar to human OA (Zhang et al., 2013; de Sousa Valente, 2019). Animals show MIA-induced pain-related behavior such as thermal hyperalgesia and mechanical allodynia that develop early after MIA injection (Ferreira-Gomes et al., 2012; Ogonna et al., 2013; Zhang et al., 2013; de Sousa Valente, 2019; Lockwood et al., 2019). The neuroinflammatory activation in DRG and spinal cord leads to plasticity changes at the spinal cord level (Ferreira-Gomes et al., 2012; Ogonna et al., 2013; Lockwood et al., 2019).

Our present study explores the efficacy of hASC secretome on pain behaviors and neuroinflammation in a MIA murine model of OA. Once assessed the presence of pain in OA mice, we injected hASC secretome in the affected paw by three different administration routes: intravenous (IV) intra-articular (IA) or intra-plantar (IPL). The effect of a single IV, IPL and IA hASC secretome injection was evaluated overtime on thermal hyperalgesia and mechanical allodynia. Neuroinflammation in nerve, DRG and spinal cord was assessed by measuring the expression levels of proinflammatory cytokines that are involved in microglia and astrocyte activation and in cell damage. Moreover, a proteomic analysis of hASC secretome unravels some of the factors that could be involved in counteracting OA-related symptoms.

2. MATERIALS AND METHODS

2.1 Animals

A total of 48 nine-week-old male C57BL/6J mice (Charles River Laboratories, Calco, Italy) were used. The animals were housed with 12-h dark/light cycle at $22 \pm 1^\circ\text{C}$ RT and

humidity of $55 \pm 10\%$ in groups of three per cages (type II—26 cm × 20 cm × 14 cm) with bedding, nesting material and enriched environment. Rodents chow consisted of standard pellet and tap water *ad libitum*. Mice were acclimatized for 1 week and handled by exposure to a passive hand, tickling and hand restraint for few minutes/day. All animal experiments complied with ARRIVE guidelines. Animal care and experimental procedures were in accordance with the International Association for the Study of Pain and European Community (E.C.L358/118/12/86) guidelines and were approved by the Animal Care and Use Committee of the Italian Ministry of Health (Authorization 180/2020 to PS). All efforts were made to minimize animal suffering and to reduce the number of animals used in accordance with the 3R principles. Correct strategies to minimize potential confounders were applied. The behavioral experiments were performed by researchers blind to treatment conditions until the completion of statistical analysis.

2.2 Induction of osteoarthritis

Mice were randomized in two experimental groups, saline-treated (controls, CTR) and MIA-treated, using the coin flipping method (Moschetti et al., 2019). Animals were anesthetized with anesthetic isoflurane plus 100% oxygen. Induction of anesthesia was performed in a chamber by 5% isoflurane and maintained with a nose with 0.7% (flow rate = 0.5-1 l/min) (Liu et al., 2014). OA was induced by a single IA injection into the right knee of 1 mg of MIA (Sigma-Aldrich, Italy) in a volume of 10µl of sterile saline (Ogbonna et al., 2013). CTR mice received an intra-articular injection of sterile saline (10µl in the right knee).

2.3 Cell harvesting and cultures

Adipose-derived stem cell (hASC) cultures were obtained from waste tissues collected at IRCCS Istituto Ortopedico Galeazzi according to the procedure PQ 7.5.125, version 4.

Written informed consent was obtained from all donors. hASC were isolated following well-established protocols (Giannasi et al., 2020). Briefly, hASC were isolated by enzymatic digestion of subcutaneous adipose tissue from patients undergoing aesthetic or prosthetic surgery, with 0.75mg/ml type I Collagenase (Worthington Biochemical Corporation, Lakewood, NJ, USA) for 30 minutes and filtering of the stromal vascular fraction. Cells were cultured in DMEM supplemented with 10% FBS (Euroclone, Italy), 2mM L-glutamine, 50U/ml penicillin and 50µg/ml streptomycin at 37°C in a humidified atmosphere with 5% CO₂. hASC were characterized as previously described (Niada et al., 2016).

2.4 Conditioned Medium (secretome) production

Conditioned medium (CM) was collected from hASC (V-VI passage) as previously described (Niada et al., 2018; Niada et al., 2020). In details, ~90% confluent hASC were washed twice with PBS, then for one hour in starving medium (phenol red-free DMEM – D1145 Sigma-Aldrich, 2mM L-glutamine, 50U/ml penicillin and 50µg/ml streptomycin), and afterwards, cultured in new fresh starving medium. After 72 hours, CM was centrifuged for 15 min at 2500g, 4°C to remove dead cells, cell debris and large apoptotic bodies. The supernatant was then centrifuged at 4000g, 4°C, inside Amicon Ultra-15 Centrifugal Filter Devices with 3kDa cut-off (Merck Millipore, Burlington, MA, USA). Protein content was measured by Bio-Rad Protein Assay Dye Reagent Concentrate (#5000006), following manufacturer's instructions. Conditioned Medium derived from 2×10^6 hASC (hASC-CM) (Brini et al., 2017), corresponding to 43.5 ± 10.5 µg of protein, was used.

2.5 Secretome treatment

Seven days after OA induction, mice in an evident state of sensory hypersensitivity (MIA-animals) were randomized into the following groups using the coin flipping method:

- MIA: no treatment

- MIA + hASC-CM/vehicle IV: animals receiving caudal tail vein injection of hASC secretome in 200µl of PBS supplemented with 2.5% heparin (vehicle) or vehicle alone.
- MIA + hASC-CM/vehicle IPL: animals receiving intraplantar injection (right paw) of hASC secretome in 15µl of vehicle or vehicle alone.
- MIA + hASC-CM/vehicle IA: animals receiving intra-articular injection (right knee) of hASC secretome in 15µl of vehicle or vehicle alone.

2.6 Behavioral test

Hypersensitivity evaluations were done before (0, basal) and 3, 7, 8, 9, 10, 14 and 21 days after OA-induction. For mechanical allodynia and thermal hyperalgesia, three different measurements were recorded for each mouse and mean calculated. Values obtained from mice of the same experimental group were then averaged and used for statistical analysis. A limping test was performed 21 days after OA induction corresponding to 14 days after hASC-CM administration.

2.6.1 Mechanical allodynia: von Frey test

Mechanical allodynia was evaluated through mechanical touch sensitivity using a blunt probe (Von Frey filament, 0.5 mm diameter, ranging up to 10 g in 10 s) on the hind-paws central plantar surface by dynamic plantar aesthesiometer (Ugo Basile, Italy). Responses to mechanical stimuli (Paw Withdrawal Thresholds, PWT) were expressed in grams (g).

2.6.2 Thermal hyperalgesia: plantar test

Thermal hyperalgesia was tested using a plantar test apparatus (Ugo Basile, Italy). The mid-plantar area of hind paws was stimulated through a constant radiant intensity heat beam (Ø 0.5 cm, Ω 20 IR) and the time (seconds, cut-off 22 s) it took to paw withdrawal was recorded (Paw Withdrawal Latency (PWL)).

2.6.3 Locomotor function: limping test

The animal was placed in a Plexiglas box (70x70x30 cm) and left free to move for 60 seconds. During the test, the animal was carefully observed by several researchers and a score from 1 to 5 was assigned, based on its behavior.

If the mouse did not limp or drag the right hind leg within this observation period, then no anomaly was highlighted and the max score of 5 was attributed. The animal behavior was graded according to the following 5 points scale:

5, no response;

4, quick limp or drag of the right leg;

3, prolonged dragging or repeated limp (more than twice) of the right leg;

2, repeated limping of the right leg with distinct dragging;

1, constant dragging of the right leg, without ever resting it.

All the researchers were blind to treatments. For each mouse, the values attributed by at least three independent researchers were averaged and used for statistical analysis.

2.7 Tissue collection

21 days after MIA, corresponding to 14 days after a single IV, IPL or IA hASC-CM treatment, mice were terminally anesthetized by isoflurane overdose. Spinal cord (L3-L6), ipsilateral DRG (L3-L6), and ipsilateral sciatic nerve and its distal branches (tibial, common peroneal and sural nerves) were isolated, snap frozen in liquid nitrogen and stored at -80°C .

2.8 RT-qPCR

RNA was extracted from homogenized tissue using TRIzol® reagent (Invitrogen, Carlsbad, USA) according to manufacturer's instruction. cDNA was obtained from 1000 ng RNA using reverse transcriptase kit LunaScript™ (BioLabs, UK). mRNA levels of interleukin-1 β (IL-1 β), interleukin 6 (IL-6), glial fibrillary acidic protein (GFAP), cluster of differentiation 68

(CD68), activating transcription factor 3 (ATF3) and toll-like receptor 4 (TLR4) (Mm00434228_m1, Mm00446190_m1, Mm01253033_m1, Mm03047343_m1, Mm00476033_m1, Mm00445274_m1) were measured with quantitative PCR by QuantStudioTM5, (Thermofisher Scientific, USA) using Taqman Gene expression assays and Luna® Universal Probe qPCR Master Mix (BioLabs, UK). The mRNA levels were normalized to GAPDH (Mm99999915_g1) and data were analyzed using the $2^{-\Delta\Delta CT}$ method. Each sample was run in duplicate alongside non-template controls.

2.9 nLC-MS/MS and data analysis

CM samples (20 µg/each) from 3 hASC populations were analyzed by nLC-MS/MS at Proteomics and Metabolomics Facility (ProMeFa - San Raffaele Scientific Institute, Milan), as previously described (Niada et al., 2020). To quantify proteins, the raw data were loaded into the MaxQuant (Cox et al., 2011) software version 1.6.1.0. Label-free protein quantification was based on the intensities of precursors. Processes/pathway analysis was performed by STRING (Szklarczyk et al., 2015) with default settings.

2.10 Statistical analysis

Experiments were designed to minimize the number of animals based on the results obtained in our previous studies (Brini et al., 2017) and on pre-study power analysis considering the antiallodynic response as the primary endpoint. Statistical analysis was performed using GraphPad Prism 6 (San Diego, CA). Normality and equal variance were checked before choosing statistical tests. Data represent mean \pm SD of 6 animals/group. Hyperalgesia and allodynia results were analyzed using Two-way repeated-measures ANOVA with Bonferroni's post hoc test. Limping scores and biochemical data were analyzed using One-way ANOVA followed by Bonferroni's test. Differences were considered significant at $p \leq 0.05$.

3. RESULTS

3.1 hASC-CM reversed MIA induced hypersensitivity

As reported in Fig. 1, the intra-articular injection of MIA elicited a significant thermal hyperalgesia (panel A) and mechanical allodynia (panel B) in the ipsilateral paw (Two-way ANOVA RM $p < 0.001$ vs CTR). Hypersensitivity was present 3 days after MIA injection and lasted for 21 days.

Seven days after MIA, when hypersensitivity was fully developed, hASC-CM or vehicle were injected by 3 different routes of administration: IA and IPL in the ipsilateral paw or IV. IV, IPL or IA vehicle administration in MIA mice did not affect thermal hyperalgesia (panel A) and mechanical allodynia (panel B). In contrast hASC-CM was able to significantly reduce thermal hyperalgesia (panel A: Two-way ANOVA RM vs respective MIA vehicle treated mice: $p < 0.001$) and mechanical allodynia (panel B: Two-way ANOVA RM vs respective MIA vehicle treated mice: $p < 0.001$) independently of the route of administration. A significant reduction of hypersensitivity was present 1 day after treatments ($p < 0.001$ vs respective MIA vehicle treated mice) and lasted up to 14 days later ($p < 0.001$ vs respective MIA vehicle treated mice). Significant differences were observed among the routes of administration. The IV hASC-CM treatment was more effective than the IPL or the IA ones in reversing thermal hyperalgesia (panel A, IV vs. IPL and IA $p < 0.001$). Moreover, the IA route was less efficacious than the IPL one in reducing thermal hyperalgesia (IA vs IPL $p < 0.001$).

As shown in panel B, the IV route was also significantly more effective than the IPL one ($p < 0.05$) and the IA one ($p < 0.001$) in reducing mechanical allodynia, starting from day 2 after administration. The IA route was less efficacious than the IPL one ($p < 0.01$). The allodynia relief induced by the IV route was complete ($p > 0.05$ vs CTR), while the thresholds of animals treated with IPL and IA hASC-CM appeared significantly lower than the control data ($p < 0.01$).

Neither PWL nor PWT measured in the contralateral paws were modified by any treatment or condition (data not shown). At day 21, an evident lameness was present in MIA mice (panel C) ($p < 0.001$ vs CTR) and only IV hASC-CM treatment significantly reduced the limping ($p < 0.05$).

3.2 Effects of hASC-CM on inflammatory markers in sciatic nerve, DRG and spinal cord of MIA treated mice

The evaluation of neuroinflammation was performed 21 days after MIA, that is 14 days after a single IV, IPL or IA hASC-CM treatment.

As reported in Fig.2, in the sciatic nerve of MIA mice, we observed a significant upregulation of all the evaluated parameters (ANOVA, $p < 0.001$ vs controls). IL-1 β and IL-6 increased levels were reduced by the IV and the IPL hASC-CM administration, but not by the IA injection (panel A, IL-1 β : $p < 0.001$ IV and IPL vs MIA; panel B IL-6: $p < 0.001$ IV vs MIA; $p < 0.05$ IPL vs MIA). GFAP upregulation was significantly blunted by IV, IPL and IA hASC-CM ($p < 0.001$ vs MIA). CD68 ($p < 0.001$ vs MIA), TLR4 ($p < 0.001$ vs MIA) and ATF3 ($p < 0.001$ IV and IPL vs MIA; $p < 0.05$ IA vs MIA) expression was also reduced by hASC-CM independently of the route of administration.

A relevant neuroinflammatory status was observed also in DRG (Fig.3). A significantly increased level of IL-1 β was present and IV, IPL, IA hASC-CM similarly decreased the cytokine expression ($p < 0.001$ vs MIA).

IV and IPL, but not IA hASC-CM also reduced CD68 ($p < 0.001$ IV vs MIA; $p < 0.05$ IPL vs MIA) and ATF3 upregulation ($p < 0.001$ IV and IPL vs MIA), while TLR4 overexpression was blunted by all hASC-CM administration routes (IV, IPL vs MIA $p < 0.001$; IA vs MIA $p < 0.01$). In this tissue, IL-6 and GFAP were not affected by MIA or treatments.

As reported in Fig.4, in the spinal cord all the neuroinflammatory markers were increased in MIA mice ($p < 0.01$ vs controls), indicating the involvement of CNS. IL-1 β and ATF3

upregulation was significantly prevented only by IV hASC-CM administration ($p < 0.01$ and $p < 0.001$ vs MIA, respectively), that was also able to partially control TLR4 activation. IL-6 and GFAP levels were similarly reduced by IV, IPL and IA hASC-CM ($p < 0.001$ vs MIA). Moreover, IV ($p < 0.001$ vs MIA), IPL and IA hASC-CM ($p < 0.01$ vs MIA) blunted CD68 expression.

3.3 Proteomic analysis of hASC-CM

To propose possible mediators of hASC-CM action, we analysed its protein content. nLC-MS/MS allowed the quantification of 671 factors in hASC-CM samples. Without considering proteins that were not present in all the samples, we selected 354 factors (Supplementary Table 1) that were analysed using STRING in order to identify enriched pathways and processes. A number of significantly enriched Reactome pathways and GO processes were identified (Supplementary Table 2 and 3). Of note, the majority of these pathways/processes are involved with the immune response. In fact, among the top 10 pathways three refer to immune system modulation (Fig.5 A-B). Gene Ontology (GO) analyses showed, as expected, an enrichment in secreted and extracellular vesicle proteins, but also strongly support the involvement of hASC-CM related factors with immune system regulation (Fig.5C).

4. DISCUSSION

Chronic pain is frequently present in OA patients, and its pharmacological treatment is never satisfactory for both scarce efficacy and side effects.

In the present work, using the well consolidated model of MIA-induced OA, we demonstrate that hASC-CM can be a valid therapeutic approach for pain relief. Our results suggest that the hASC-CM effect is likely mediated by the modulation of neuroinflammation in the peripheral and central nervous system.

During experimental OA, joint afferents typically expand their receptive fields to areas adjacent to the injected joint; the same expansion of receptive fields and reduction of mechanical thresholds around the joint area have been observed in OA patients (Miller and Malfait, 2017). As expected, after MIA injection in the joint we observed the development of referred pain, expressed as thermal hyperalgesia and mechanical allodynia in the ipsilateral paw. Hypersensitivity appeared in 3 days and remained stable up to 21 days after MIA.

We decided to treat MIA animals with hASC-CM 7 days after OA induction, once hypersensitivity was stable and became comparable to chronic pain even though the animals were not in an end-stage disease yet.

Independently of the route of administration, a single hASC-CM treatment induced a fast and long lasting pain relief, still present 14 days later. The rapid and persistent analgesic effect of a single hASC-CM administration is a common feature, since it was observed in the treatment of different types of chronic pain, such as neuropathic and inflammatory pain in the rodent (Guo et al., 2011; Praveen Kumar et al., 2019; Brini et al., 2017).

hASC-CM was effective after IPL, IA and IV injection. However, IV administration was significantly more efficacious than the others were, while the IA one was the less active. It is important to point out that the evoked response to the mechanical stimulus was completely abolished after IV hASC-CM administration. This aspect is relevant since in OA patients a clear mechanical component of pain is predominant, and a quantitative sensory testing has shown the presence of reduced thresholds to mechanical stimuli both at the affected joint and at remote sites (Suokas et al., 2012). Moreover, the IV secretome administration significantly improved also spontaneous locomotor activity, reducing limping behavior.

In recent years MSCs and, to a lesser extent, their secretome have been increasingly considered as promising tools in the regenerative medicine field. Nevertheless, several

aspects concerning their clinical application still need to be clarified, such as the choice of the best route of administration in the different pathological conditions. In joint pathology, IA administration represents the gold standard choice for orthopedic surgeons. However, our results indicate that IA, although effective, is the least efficacious route of administration for treating OA-associated chronic pain. Conversely, in our OA model, the systemic injection of hASC-CM represents the most effective treatment. These observations lead us to hypothesize that the antihyperalgesic and antiallodynic action is not only exerted in the joint, but rather on peripheral and central nervous system where the events seem to lead to pain sensitization.

Chronic pain is often characterized by the presence of neuroinflammation in both peripheral and central nervous system, and a pathological cross-talk between neuronal and non neuronal cells is a common substrate to several chronic pain conditions (de Sousa Valente, 2019). Our data confirm and expand the concept of an overt neuroinflammation affecting the nerve, the DRG and the spinal cord also in a mouse model of OA pain. In the literature, there are no studies/observations at the nerve level in the MIA mouse model. Considering that pain measurements are performed at the paw level (referred pain) and that the sciatic nerve and its distal afferents (tibial, common peroneal and sural nerves) are those that innervate the paw, we decided to analyze neuroinflammation in the sciatic nerve. In this tissue, we observed an unexpected overexpression of inflammatory cytokines and macrophage markers. Activated Schwann cells or infiltrating macrophages could be responsible for the increase of inflammatory markers in the sciatic nerves and may be a consequence of demyelination phenomena (Muley et al., 2017). We also detected in this tissue a significant increase of ATF3. The relevant increase of ATF3 in the nerve can be attributed to the fact that it can be upregulated in several cell types. In fact both Schwann cells and CD68 positive cells

infiltrating the damaged tissue can overexpress it, and it has also been reported that ATF3 could be retrogradely transported from DRG to axons (Hunt et al., 2012).

Further experiments on nerve morphology and conduction are needed to understand the role of neuroinflammation of the sciatic nerve in OA chronic pain. Also in DRG, we observed an overexpression of mRNA for macrophage/microglia markers such as CD68, TLR4 and for the proinflammatory cytokine IL-1 β . Our data suggest a crucial role of TLR4 and of infiltrated macrophages in PNS; upon activation, these cells release a broad spectrum of proinflammatory mediators like cytokines and chemokines contributing to damage and sensitizing processes (Miller and Malfait, 2017). The sensitization process proceeds to the spinal cord, where we demonstrated microglia activation and IL-1 β overexpression, in agreement with previous reports (Im et al., 2010; de Sousa Valente, 2019).

In contrast with the established role of microglia in the development of hypersensitivity in the MIA model of OA, the role of astrocytes is less clear, indeed studies reported either a lack of astrocyte response (Ogbonna et al., 2013) or an increase of GFAP (Lin et al., 2017). Our results about the increase of GFAP mRNA both in nerve and spinal cord, support the hypothesis that, 21 days after MIA injection, the activation of Schwann cells in the nerve and of astrocytes in the spinal cord contribute to the transition to chronic pain. Moreover, also ATF3 mRNA, a marker of neuronal damage, is consistently overexpressed in the nervous tissues. This confirms previous data on its activation in rat models of OA (Ivanavicius et al., 2007; Thakur et al., 2012; Ferreira-Gomes et al., 2012), that was not formerly described in the mouse (Ogbonna et al., 2013). One explanation could be the different time point of the analysis, since our data refer to 21 days after MIA injection, when the hypersensitivity is chronic.

Treatment with hASC-CM has a relevant positive impact on the neuroinflammatory parameters. According to what we observed for pain relief, the IV route of administration is

also the most effective one in relieving neuroinflammation. In fact, proinflammatory cytokines, macrophage marker upregulation, microgliosis, astrocyte activation and ATF3 overexpression are reduced to physiological levels after IV treatment. Differently, after IPL and IA hASC-CM administration the reduction of neuroinflammation, although still evident, does not affect all the analyzed markers and mediators. For example, the IA treatment fails to normalize ATF3 upregulation in all the tissues or reestablish basal levels of TLR4 and IL-1 β in spinal cord. Therefore, we think that there is a reasonable correlation between the degree of efficacy of the three tested routes of administration to ameliorate painful behaviors and the control of neuroinflammation in the peripheral and central nervous system.

Considering these results, we are confident enough to hypothesize that the effect of hASC-CM is exerted mainly in the nervous system rather than directly in the joint.

The biologically active substances contained in the hASC-CM (cytokines, chemokines, cell adhesion molecules, lipid mediators, growth factors, hormones, exosomes, microvesicles, etc.) can activate/deactivate specific signaling pathways in the peripheral and central nervous system with a final protective outcome (Harrell et al., 2019; Praveen Kumar et al., 2019). Furthermore, the lasting antiallodynic and antihyperalgesic effect of hASC-CM may favor the hypothesis of a reprogramming of the immune and neuronal environments that, once activated, change the course of neuroinflammation and pain establishment in this OA model. We would like to highlight that our study was performed in a mouse model.

Although a pain relief lasting 14 days after a single treatment is very relevant in the mouse, we cannot speculate on the duration of the effect in humans, as in patients OA and associated pain may last for several years. However, the useful and surprising long lasting effect of hASC-CM has been already described in other rodent models of pathological conditions, such as diabetic neuropathy and nephropathy (Brini et al., 2017), liver disease,

urological dysfunction and Alzheimer disease (Mita et al., 2015; Lee et al., 2015; Yiou et al., 2016).

The present study is focused on the secretome, that represents a novel and safer approach, and we did not directly compare its efficacy with that of hASCs. In a preliminary experiment in this MIA model we evaluated the effect of hASCs only on hyperalgesia and the results were similar to those reported for secretome (data not shown). Previous work from our group demonstrated that IV hASC-CM and hASCs similarly relieved pain and neuroinflammation in a murine model of diabetic neuropathy, suggesting that secretome may mimic the effects of the cell therapy on pain and neuroinflammation (Brini et al., 2017). However, considering the studies that indicate a reparative effect of IA injected MSCs (Jayaram et al., 2019; Doyle et al., 2020), together with the evidence of a certain, even though limited, engraftment of these cells in the OA joint (Satué et al., 2019; Enomoto et al., 2020; Park et al., 2017), and their plasticity and ability to modify their secretome in response to the environment (e.g. inflammatory mediators) (Barry, 2019), we cannot rule out that cells would be more effective than secretome when injected locally in the joint. It can be hypothesized that cells and secretome may indeed have synergistic or complementary effects, but further experiments are needed in this direction.

To figure out a cocktail of possible mediators involved in the hASC-CM anti-neuroinflammatory action, we analysed its proteomic profile. The investigation of the enriched pathways and processes indicated that ten out of the top twenty processes are associated with immunity, and 101 factors were identified as associated with immune regulation. Several factors present interesting features related to neuroinflammation down modulation. ADAM10 has been shown to repress hippocampal neuroinflammation (Zhu et al., 2018). Annexin is a key player in the resolution of peripheral inflammation and act at CNS level by modulating microglia activity and preventing the production of proinflammatory mediators (McArthur et al., 2010). Clusterin is involved in neuronal

protection (Gregory et al., 2017) and it might modulate neuroinflammation by suppressing complement activation. Gelsolin possesses analgesic and anti-inflammatory properties (Gupta et al., 2015). Pentraxin 3, an essential mediator of anti-inflammatory and protective effects in peripheral inflammatory conditions also exerts its function in CNS reducing neuroinflammation (Rajkovic et al., 2019). At last, Tissue-Inhibitor-Metalloproteases (TIMPs) might play a fundamental role in dampening down pain. This could be explained by the known fine tuning between Metalloproteases (MMPs) and TIMPs activity that in pathological inflammatory status is often compromised. In the pain context, TIMPs have been shown to reduce mechanical and thermal hypersensitivity following nerve damage by inhibiting MMPs activity (Kawasaki et al., 2008; Knight et al., 2019).

Exosomes are also present in hASC-CM (Niada et al., 2019), and they carry specific mRNA or miRNA, which could potentiate the reparative and healing process of injured tissues. Although it is possible that for different pathological conditions, diverse mediators may be responsible for the hASC-CM beneficial effect, we think that what makes the secretome unique is indeed the simultaneous presence of all these multiple factors. Of note, cell secretome composition could be modified in order to enhance its efficacy.

Multiple priming strategies, such as cytokine, pharmacological or chemical treatment and hypoxia, are currently under investigation (Noronha et al., 2019). In the light of Dazzi's group and others findings, (Galleu et al., 2017; Liu et al., 2020) the induction of cell apoptosis and the inclusion of all the apoptotic bodies in conditioned medium might represent a good strategy, too.

The interest in the use of stem cell-derived secretome rather than stem cells themselves for the treatment of inflammatory and degenerative diseases is rapidly increasing. Indeed MSC-secretome bypasses many limitations of MSC-based therapy, including unwanted differentiation and potential activation of allogeneic immune response (Lukomska et al., 2019; Volarevik et al., 2018). Several important advantages of secretome compared with

its cell-based counterpart have to be considered including a reduced product variability, a higher reproducibility, an easy and less cost effective storage, together with a safer profile, and dosage (Harrell et al., 2019; Praveen Kumar et al., 2019).

Although the use of secretome has already reached patients (Katagiri et al., 2016; 2017) and no adverse effects were described, we are also aware that several steps are needed before proceeding to large-scale use of secretome for human treatment. Current Good Manufacturing Practices (cGMP) compliant protocols for the preparation, the storage, and the stability of the MSC secretome, together with control parameters are needed. Moreover, optimal protein concentration of the dose, administration route, and frequency and volume of injection, must still be determined in the perspective of a clinical translation.

5.0 CONCLUSION

We demonstrate that hASC-CM is a valid treatment option for controlling OA related hypersensitivity, exerting a rapid and lasting relief of painful symptoms. Several routes of administration may be exploited, although the systemic injection appears to be the most active in our MIA model of OA. The mechanisms at the basis of the effects can be ascribed to the ability of hASC-CM to positively modulate the neuroinflammation that sustains peripheral and central sensitization in peripheral and central nervous system. In the future, we will use our model to evaluate the efficacy of cocktails of selected factors, soluble or trapped in extracellular vesicles in order to provide a future clinical treatment for OA.

Acknowledgement

Financial support: This research was partly funded by the Italian Ministry of Health (Ricerca Corrente L1038 and L1039 of IRCCS Istituto Ortopedico Galeazzi).

Moschetti Giorgia was supported by the cycle XXXII of the doctorate in Experimental and Clinical Pharmacological Sciences, Università degli Studi di Milano, Milano, Italy.

LEGENDS

Fig. 1. Allodynia and hyperalgesia. Development of thermal hyperalgesia (panel A), mechanical allodynia (panel B) and limping (panel C), following MIA intra-articular administration (right knee) and the effect of vehicle or hASC-CM administration in MIA mice at day 7 after MIA by three different routes: intravenous (IV), intraplantar (IPL) and intra-articular (IA). Data are presented as the mean \pm SD of 6 mice per group. Statistical analysis of thermal hyperalgesia and mechanical allodynia was performed by means of Two-way ANOVA for repeated measures followed by the Bonferroni's post test. Treatment: F (7, 35) panel A= 592.2, $p<0.0001$; panel B=205.1, $p<0.0001$; Time: F (7, 35) panel A=1676, $p<0.0001$; panel B=368.7, $p<0.0001$; Interaction: F (49,245) panel A=86.27, $p<0.0001$; panel B=24.99, $p<0.0001$. Statistical analysis of limping was performed by One-way ANOVA followed by Bonferroni's post test, F (4, 25) =9.316, $p<0.0001$.

*** $p<0.001$, ** $p<0.01$, * $p<0.05$ vs CTR (intra-articular treated with saline), °°° $p<0.001$, ° $p<0.05$ hASC-CM vs vehicle by the same route of administration in MIA mice, #### $p<0.001$, ## $p<0.01$, # $p<0.05$ vs IV hASC-CM, +++ $p<0.001$, ++ $p<0.05$ vs IPL hASC-CM.

Fig. 2. Biochemical evaluation in sciatic nerve. mRNA levels of neuroinflammatory markers (IL-1 β , IL-6, GFAP, CD68, ATF3 and TLR4 reported in panels a, b, c, d, e, f, respectively) were measured in ipsilateral sciatic nerve using Real Time-qPCR. Evaluations were performed 21 days after MIA intra-articular administration (right knee), corresponding to 14 days after hASC-CM injection. hASC-CM was administered to MIA-mice by three different routes: intravenous (IV), intraplantar (IPL), intra-articular (IA). Results were expressed in relation to GAPDH and presented as fold-increases over the levels of CTR-mice. Data are expressed as the mean \pm SD from 6 mice per group. Statistical analysis was performed by One-way ANOVA followed by Bonferroni's post test. F(4,25) IL-1 β =70.59,

$p < 0.0001$; IL-6=16.80, $p < 0.0001$; GFAP=48.95, $p < 0.0001$; CD68 =49.88, $p < 0.0001$, ATF3=33.80, $p < 0.0001$; TLR4 =17.88, $p < 0.0001$. *** $p < 0.001$, ** $p < 0.01$, * $p < 0.05$ vs CTR (intra-articular saline treatment); °°° $p < 0.001$, ° $p < 0.05$ vs MIA ; ### $p < 0.001$, # $p < 0.05$ vs IV hASC-CM, +++ $p < 0.001$, ++ $p < 0.01$ vs IPL hASC-CM.

Fig. 3. Biochemical evaluation in DRG. mRNA levels of neuroinflammatory markers (IL-1 β , IL-6, GFAP, CD68, ATF3 and TLR4 reported in panels a, b, c, d, e, f respectively) were measured in ipsilateral DRG by using Real Time-qPCR. Evaluations were performed 21 days after MIA intra-articular administration (right knee), corresponding to 14 days after hASC-CM injection. hASC-CM was administered to MIA-mice by three different routes: intravenous (IV), intraplantar (IPL), intra-articular (IA). Results were expressed in relation to GAPDH and presented as fold-increases over the levels of CTR-mice. Data are expressed as the mean \pm SD from 6 mice per group. Statistical analysis was performed by One-wayANOVA followed by Bonferroni's post test. F(4,25) IL-1 β =13.22, $p < 0.0001$; IL-6=5.172, $p = 0.0035$; GFAP=2.886, $p = 0.0430$; CD68=13.99, $p < 0.0001$; ATF3=23.54, $p < 0.0001$; TLR4=40.66, $p < 0.0001$. *** $p < 0.001$, ** $p < 0.01$, * $p < 0.05$ vs CTR (intra-articular saline treatment), °°° $p < 0.001$, ° $p < 0.01$, ° $p < 0.05$ vs MIA, ### $p < 0.001$, ## $p < 0.01$, # $p < 0.05$ vs IV hASC-CM, ++ $p < 0.01$ vs IPL hASC-CM.

Fig. 4. Biochemical evaluation in spinal cord. mRNA levels of neuroinflammatory markers (IL-1 β , IL-6, GFAP, CD68, ATF3 and TLR4 reported in panels a, b, c, d, e, f respectively) were measured in spinal cord by using Real Time-qPCR. Evaluations were performed 21 days after MIA intra-articular administration (right knee), corresponding to 14 days after hASC-CM injection. hASC-CM was administered to MIA-mice by three different routes: intravenous (IV), intraplantar (IPL), intra-articular (IA). Results were expressed in relation to GAPDH and presented as fold-increases over the levels of CTR-mice. Data are

expressed as the mean \pm SD from 6 mice per group. Statistical analysis was performed by One-wayANOVA followed by Bonferroni's post test. Treatment: F(4,25) IL-1 β =6.895, p=0.0007; IL-6=49.81, p<0.0001; GFAP=35.03, p<0.0001; CD68=7.434, p=0.0004; ATF3=13.42, p<0.0001; TLR4=6.209, p=0.0013. ***p<0.001, **p<0.01, *p<0.05 vs CTR (intra-articular saline treatment), °°°p<0.001, °°p<0.01, vs MIA, #p<0.05 vs IV hASC.

Fig. 5. STRING analysis of hASC-CM proteome. Top 10 Reactome Pathways associated to hASC-secreted factors (panel A). Protein-protein interactions of the 101 factors involved in Neutrophil degranulation (HSA-6798695), Innate Immune System (HSA-168249) and Immune System (HSA-168256) (panel B). Gene Ontology analyses of hASC-CM proteins (panel C). Top 20 processes were selected on the basis of false discovery rate (FDR) p value (Log FDR p value are reported as orange bars). Fold enrichment was calculated as follows: fold enrichment = (observed protein count/ hASC-CM characteristic proteins)/ (background gene count/total gene number) and it is reported as blue bars.

Supplementary Table 1. Lists of proteins (gene names are reported) used for STRING analyses.

Supplementary Table 2. STRING Reactome pathway analyses of hASC-CM proteins, ordered by FDR p value.

Supplementary Table 3. STRING Gene Ontology analyses of hASC-CM proteins, ordered by FDR value. Fold Enrichment: (n/m)/ (N/M); n= proteins identified in all hASC-CM sample (supplementary table 1) belonging to the pathway/process; m= protein list; N= all genes/proteins belonging to the pathway/process; M= patall genes/proteins (universe). Benjamini: benjamini p-value.

REFERENCES

- Alshami, A.M., 2014. Knee osteoarthritis related pain: a narrative review of diagnosis and treatment. *Int J Health Sci (Quassim)*. 8(1):85-104. (Review) DOI: 10.12816/0006075
- Arendt-Nielsen, L., Nie, Hongling., Laursen, M.B., Laursen, B.S., Pascal, M., Simonsen, H.O., Graven-Nielsen, T., 2010. Sensitization in patients with painful knee osteoarthritis. *Pain*. 149(3):573-581.
- Barr, A.J., Campbell, T.M., Hopkinson, D., Kingsbury, S.R., Bowes, M.A., Conaghan, P.G., 2015. A systematic review of the relationship between subchondral bone features, pain and structural pathology in peripheral joint osteoarthritis. *Arthritis Res Ther*. 17(1):228. (Review) DOI: 10.1186/s13075-015-0735-x
- Barry, F., 2019. MSC Therapy for Osteoarthritis: An Unfinished Story. *J Orthop Res*, 37, 1229-1235. DOI: 10.1002/jor.24343
- Bedson J., Croft P.R., 2008. The discordance between clinical and radiographic knee osteoarthritis: a systematic search and summary of the literature. *BMC Musculoskelet Disord*. 9:116. DOI: 10.1186/1471-2474-9-116.
- Brini, A.T., Amodeo, G., Ferreira, L.M., Milani, A., Niada, S., Moschetti, G., Franchi, S., Borsani, E., Rodella, L.F., Panerai, A.E., Sacerdote, P., 2017. Therapeutic effect of human adipose-derived stem cells and their secretome in experimental diabetic pain. *Sci Rep*. 7(1):9904. DOI: 10.1038/s41598-017-09487-5
- Caplan, A.I., 2017. Mesenchymal stem cells: time to change the name! *Stem Cells Transl Med*. 6(6):1445-1451. DOI: 10.1002/sctm.17-0051
- Cox, J., Neuhauser, N., Michalski, A., Scheltema, R.A., Olsen, J.V., Mann, M., 2011. Andromeda: a peptide search engine integrated into the MaxQuant environment. *J Proteome Res* 2011; 10(4):1794-1805. DOI: 10.1021/pr101065j
- Crivelli, B., Chlapanidas, T., Perteghella, S., Lucarelli, E., Pascucci, L., Brini, A.T., Ferrero, I., Marazzi, M., Pessina, A., Torre, M.L., Italian Mesenchymal Stem Cell Group (GISM), 2017. Mesenchymal stem/stromal cell extracellular vesicles: From active principle to next generation drug delivery system. *J Control Release*. 262:104-117. (Review) DOI: 10.1016/j.jconrel.2017.07.023

- de Girolamo, L., Niada, S., Arrigoni, E., Di Giancamillo, A., Domeneghini, C., Dadsetan, M., Yaszemski, M.J., Gastaldi, D., Vena, P., Taffetani, M., Zerbi, A., Sansone, V., Peretti, G.M., Brini, A.T., 2015. Repair of osteochondral defects in the minipig model by OPF hydrogel loaded with adipose-derived mesenchymal stem cells. *Regen Med.* 10(2):135-151. DOI: 10.2217/rme.14.77
- de Sousa Valente, J., 2019. The pharmacology of pain associated with the monoiodoacetate model of osteoarthritis. *Front Pharmacol.* 10:974. (Review) DOI: 10.3389/fphar.2019.00974
- Doyle, E. C., Wragg, N. M. & Wilson, S. L., 2020. Intraarticular injection of bone marrow-derived mesenchymal stem cells enhances regeneration in knee osteoarthritis. *Knee Surg Sports Traumatol Arthrosc*, 28, 3827-3842. DOI: 10.1007/s00167-020-05859-z
- Enomoto, T., Akagi, R., Ogawa, Y., Yamaguchi, S., Hoshi, H., Sasaki, T., Sato, Y., Nakagawa, R., Kimura, S., Ohtori, S. & Sasho, T., 2020. Timing of Intra-Articular Injection of Synovial Mesenchymal Stem Cells Affects Cartilage Restoration in a Partial Thickness Cartilage Defect Model in Rats. *Cartilage*, 11, 122-129. DOI: 10.1177/1947603518786542
- Felson D.T., 2013. Osteoarthritis as a disease of mechanics. *Osteoarthritis Cartilage.* 21(1):10-5. DOI: 10.1016/j.joca.2012.09.012.
- Ferreira-Gomes, J., Adães, S., Sousa, R.M., Mendonça, M., Castro-Lopes, J.M., 2012. Dose-dependent expression of neuronal injury markers during experimental osteoarthritis induced by monoiodoacetate in the rat. *Mol Pain.* 8:50. DOI: 10.1186/1744-8069-8-50
- Galleu, A., Riffo-Vasquez, Y., Trento, C., Lomas, C., Dolcetti, L., Cheung, T. S., Von Bonin, M., Barbieri, L., Halai, K., Ward, S., Weng, L., Chakraverty, R., Lombardi, G., Watt, F. M., Orchard, K., Marks, D. I., Apperley, J., Bornhauser, M., Walczak, H., Bennett, C. & Dazzi, F. 2017. Apoptosis In Mesenchymal Stromal Cells Induces In Vivo Recipient-Mediated Immunomodulation. *Sci Transl Med*, 9.
- Giannasi, C., Niada, S., Magagnotti, C., Ragni, E., Andolfo, A., Brini, A.T., 2020. Comparison of two ASC-derived therapeutics in an in vitro OA model: secretome versus extracellular vesicles. *Stem Cell Res Ther.* 11(1):521. DOI: 10.1186/s13287-020-02035-5.

- Gregory, J.M., Whiten, D.R., Brown, R.A., Barros, T.P., Kumita, J.R., Yerbury, J.J., Satapathy, S., McDade, K., Smith, C., Luheshi, L.M., Dobson, C.M., Wilson, M.R., 2017. Clusterin protects neurons against intracellular proteotoxicity. *Acta Neuropathol Commun.* 5(1):81. DOI: 10.1186/s40478-017-0481-1
- Grubb, B.D., Stiller, R.U., Schaible, H.G., 1993. Dynamic changes in the receptive field properties of spinal cord neurons with ankle input in rats with chronic unilateral inflammation in the ankle region. *Exp Brain Res.* 92(3):441-452. DOI: 10.1007/BF00229032
- Guo, W., Wang, H., Zou, S., Gu, M., Watanabe, M., Wei, F., Dubner, R., Huang, G.T., Ren, K., 2011. Bone marrow stromal cells produce long-term pain relief in rat models of persistent pain. *Stem Cells.* 29(8):1294-303. DOI: 10.1002/stem.667
- Gupta, A.K., Parasar, D., Sagar, A., Choudhary, V., Chopra, B.S., Garg, R., Ashish, Khatri, N., 2015. Analgesic and anti-inflammatory properties of gelsolin in acetic acid induced writhing, tail immersion and carrageenan induced paw edema in mice. *PLoS One* 10(9):e0135558. DOI: 10.1371/journal.pone.0135558
- Harrell, C.R., Fellabaum, C., Jovicic, N., Djonov, V., Arsenijevic, N., Volarevic, V., 2019. Molecular mechanisms responsible for therapeutic potential of mesenchymal stem cell-derived secretome. *Cells.* 8(5):467. (Review) DOI: 10.3390/cells8050467
- Haywood, A.R., Hatway, G.J., Chapman, V., 2018. Differential contribution of peripheral and central mechanisms to pain in a rodent model of osteoarthritis. *Sci Rep.* 8(1):7122. DOI: 10.1038/s41598-018-25581-8
- Hunt, D., Raivich, G., Anderson, P.N., 2012. Activating transcription factor 3 and the nervous system. *Front Mol Neurosci.* 5:7. DOI: 10.3389/fnmol.2012.00007.
- Hunter, D.J., Schofield, D., Callander, E., 2014. The individual and socioeconomic impact of osteoarthritis. *Nat Rev Rheumatol.* 10(7):437-441. (Review) DOI: 10.1038/nrrheum.2014.44
- Im, H.J., Kim, J.S., Li, X., Kotwal, N., Sumner, D.R., van Wijnen, A.J., Davis, F.J., Yan, D., Levine, B., Henry, J.L., Desevré, J., Kroin, J.S., 2010. Alteration of sensory neurons

and spinal response to an experimental osteoarthritis pain model. *Arthritis Rheum.* 62(10):2995-3005. DOI: 10.1002/art.27608

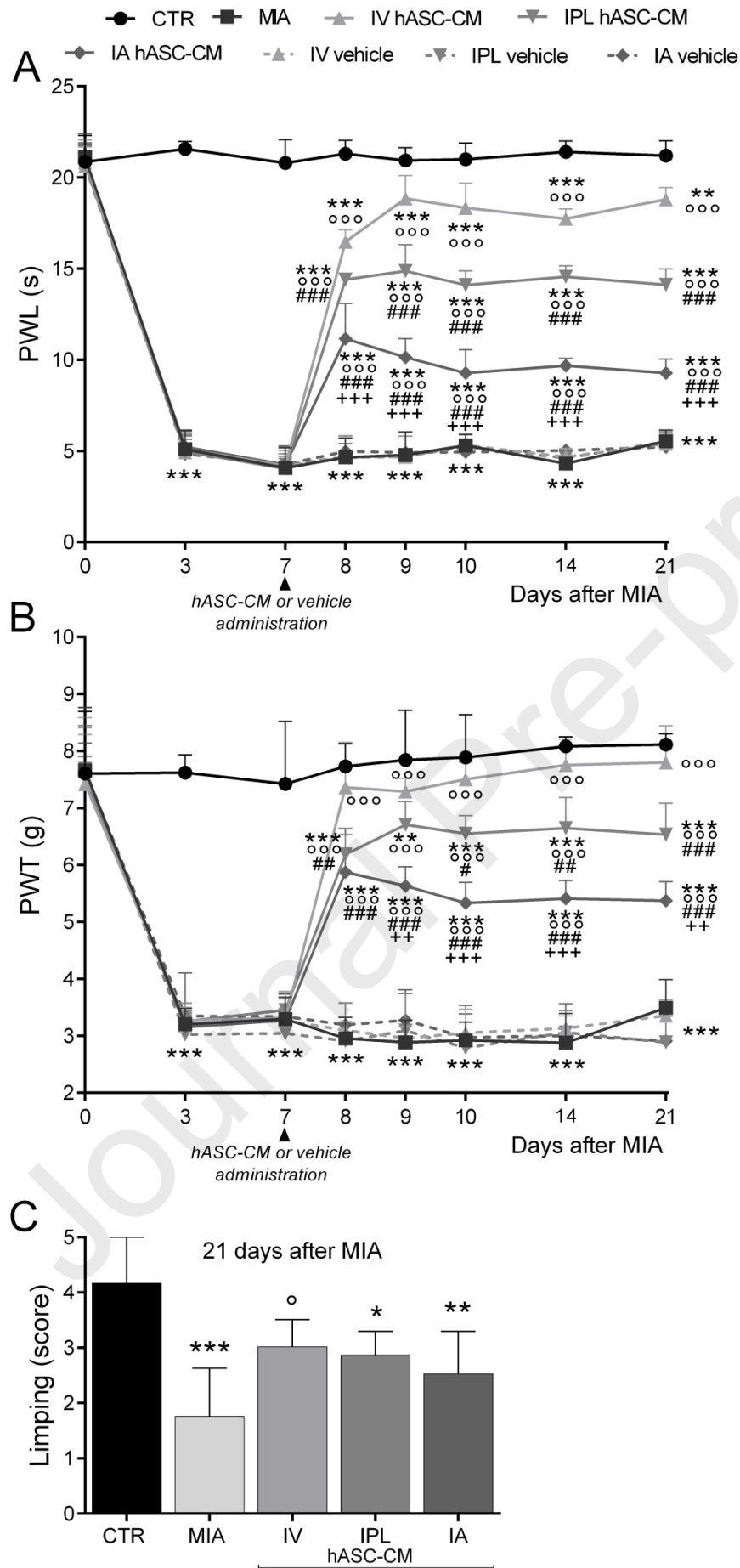
- Ivanavicius, S.P., Ball, A.D., Heapy, C.G., Westwood, F.R., Murray, F., Read, S.J., 2007. Structural pathology in a rodent model of osteoarthritis is associated with neuropathic pain: increased expression of ATF-3 and pharmacological characterisation. *Pain.* 128(3):272-82. DOI: 10.1016/j.pain.2006.12.022
- Jayaram, P., Ikpeama, U., Rothenberg, J. B. & Malanga, G. A., 2019. Bone Marrow-Derived and Adipose-Derived Mesenchymal Stem Cell Therapy in Primary Knee Osteoarthritis: A Narrative Review. *Pm r*, 11, 177-191. DOI: 10.1016/j.pmrj.2018.06.019
- Katagiri, W., Osugi, M., Kawai, T., Hibi, H., 2016. First-in-human study and clinical case reports of the alveolar bone regeneration with the secretome from human mesenchymal stem cells. *Head Face Med.* 12:5. DOI: 10.1186/s13005-016-0101-5.
- Katagiri, W., Watanabe, J., Toyama, N., Osugi, M., Sakaguchi, K., Hibi, H., 2017. Clinical Study of Bone Regeneration by Conditioned Medium From Mesenchymal Stem Cells After Maxillary Sinus Floor Elevation. *Implant Dent.* 26(4):607-612. DOI: 10.1097/ID.0000000000000618.
- Kawasaki, Y., Xu, Z.Z., Wang, X., Park, J.Y., Zhuang, Z.Y., Tan, P.H., Gao, Y.J., Roy, K., Corfas, G., Lo, E.H., Ji, R.R., 2008. Distinct roles of matrix metalloproteases in the early- and late-phase development of neuropathic pain. *Nat Med.* 14(3):331-336. DOI: 10.1038/nm1723
- Knight, B.E., Kozlowski, N., Havelin, J., King, T., Crocker, S.J., Young, E.E., Baumbauer, K.M., 2019. TIMP-1 Attenuates the development of inflammatory pain through mmp-dependent and receptor-mediated cell signaling mechanisms. *Front Mol Neurosci.* 12:220. DOI: 10.3389/fnmol.2019.00220
- Lee, S.K., Lee, S.C., Kim, S.J., 2015. A novel cell-free strategy for promoting mouse liver regeneration: utilization of a conditioned medium from adipose-derived stem cells. *Hepatol Int.* 9:310–320. DOI: 10.1007/s12072-014-9599-4

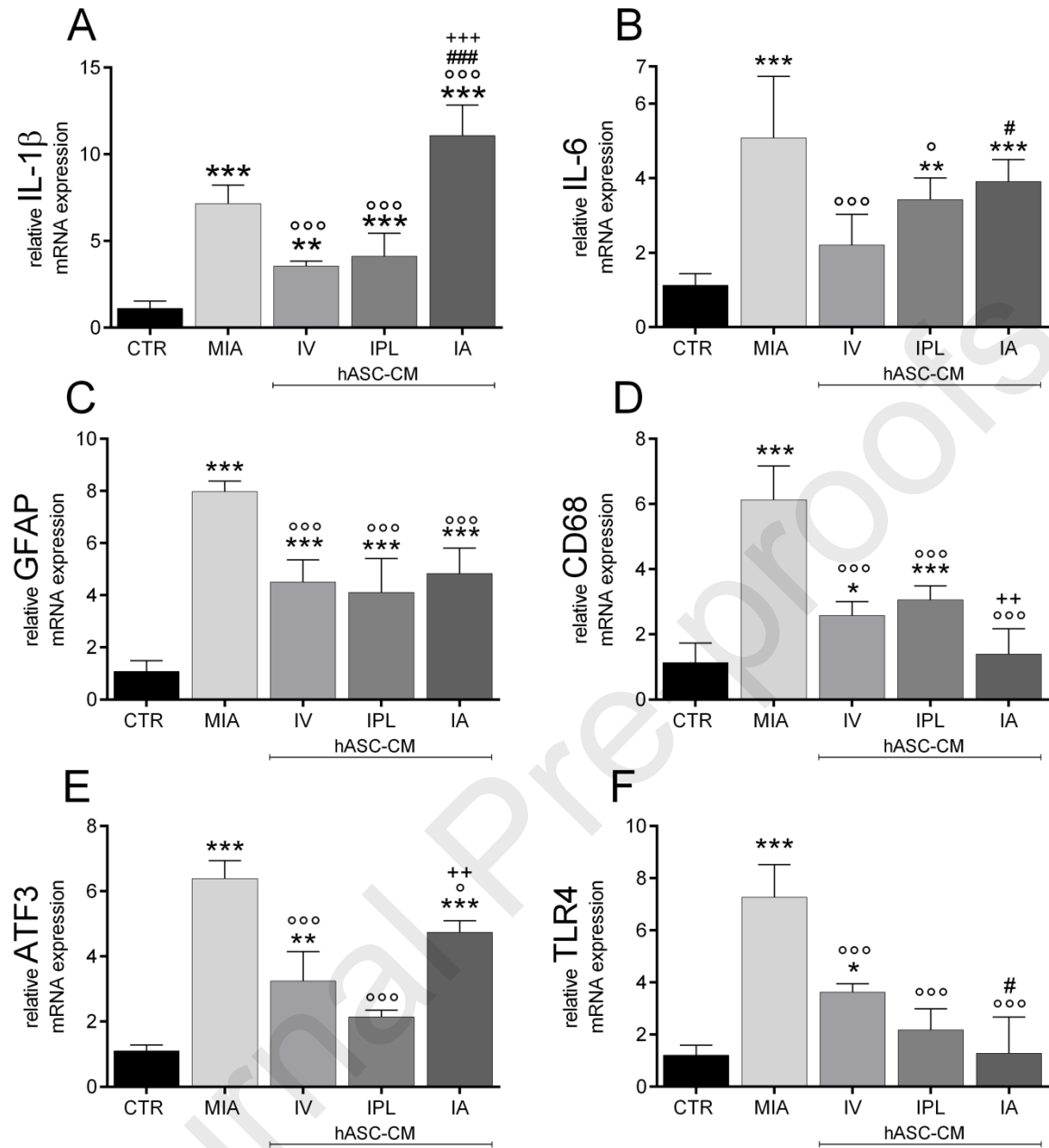
- Lin, Y., Liu, L., Jiang, H., Zhou, J., Tang, Y., 2017. Inhibition of interleukin-6 function attenuates the central sensitization and pain behavior induced by osteoarthritis. *Eur J Pharmacol.* 811:260-267. DOI: 10.1016/j.ejphar.2017.06.032
- Liu, J., Wang, P., Zhang, X., Zhang, W., Gu, G., 2014. Effects of different concentration and duration time of isoflurane on acute and long-term neurocognitive function of young adult C57BL/6 mouse. *Int J Clin Exp Pathol.* 7(9):5828-5836.
- Liu, J., Qiu, X., Lv, Y., Zheng, C., Dong, Y., Dou, G., Zhu, B., Liu, A., Wang, W., Zhou, J., Liu, S., Gao, B. & Jin, Y. 2020. Apoptotic bodies derived from mesenchymal stem cells promote cutaneous wound healing via regulating the functions of macrophages. *Stem Cell Res Ther*, 11, 507.
- Lockwood, S.M., Lopes, D.M., McMahon, S.B., Dickenson, A.H., 2019. Characterisation of peripheral and central components of the rat monoiodoacetate model of osteoarthritis. *Osteoarthritis Cartilage.* 27(4):712-722. DOI: 10.1016/j.joca.2018.12.017
- Lukomska, B., Stanaszek, L., Zuba-Surma, E., Legosz, P., Sarzynska, S., Drela, K., 2019. Challenges and Controversies in Human Mesenchymal Stem Cell Therapy. *Stem Cells International.* vol. 2019, Article ID 9628536, 10 pages, 2019. DOI: 10.1155/2019/9628536
- Mandl, L.A., 2019. Osteoarthritis year in review 2018: clinical. *Osteoarthritis Cartilage* 27(3):359-364. (Review) DOI: 10.1016/j.joca.2018.11.001
- McArthur, S., Cristante, E., Paterno, M., Christian, H., Roncaroli, F., Gillies, G.E., Solito, E., 2010. Annexin A1: a central player in the anti-inflammatory and neuroprotective role of microglia. *J Immunol.* 185(10):6317-6328. DOI: 10.4049/jimmunol.1001095
- Miller, R.E., Malfait, A.M., 2017. Osteoarthritis pain: What are we learning from animal models?. *Best Pract Res Clin Rheumatol.* 31(5):676-687. (Review) DOI: 10.1016/j.berh.2018.03.003
- Mita, T., Furukawa-Hibi, Y., Takeuchi, H., Hattori, H., Yamada, K., Hibi, H., Ueda, M., Yamamoto, A., 2015. Conditioned medium from the stem cells of human dental pulp improves cognitive function in a mouse model of Alzheimer's disease. *Behav Brain Res.* 293:189–197. DOI: 10.1016/j.bbr.2015.07.043

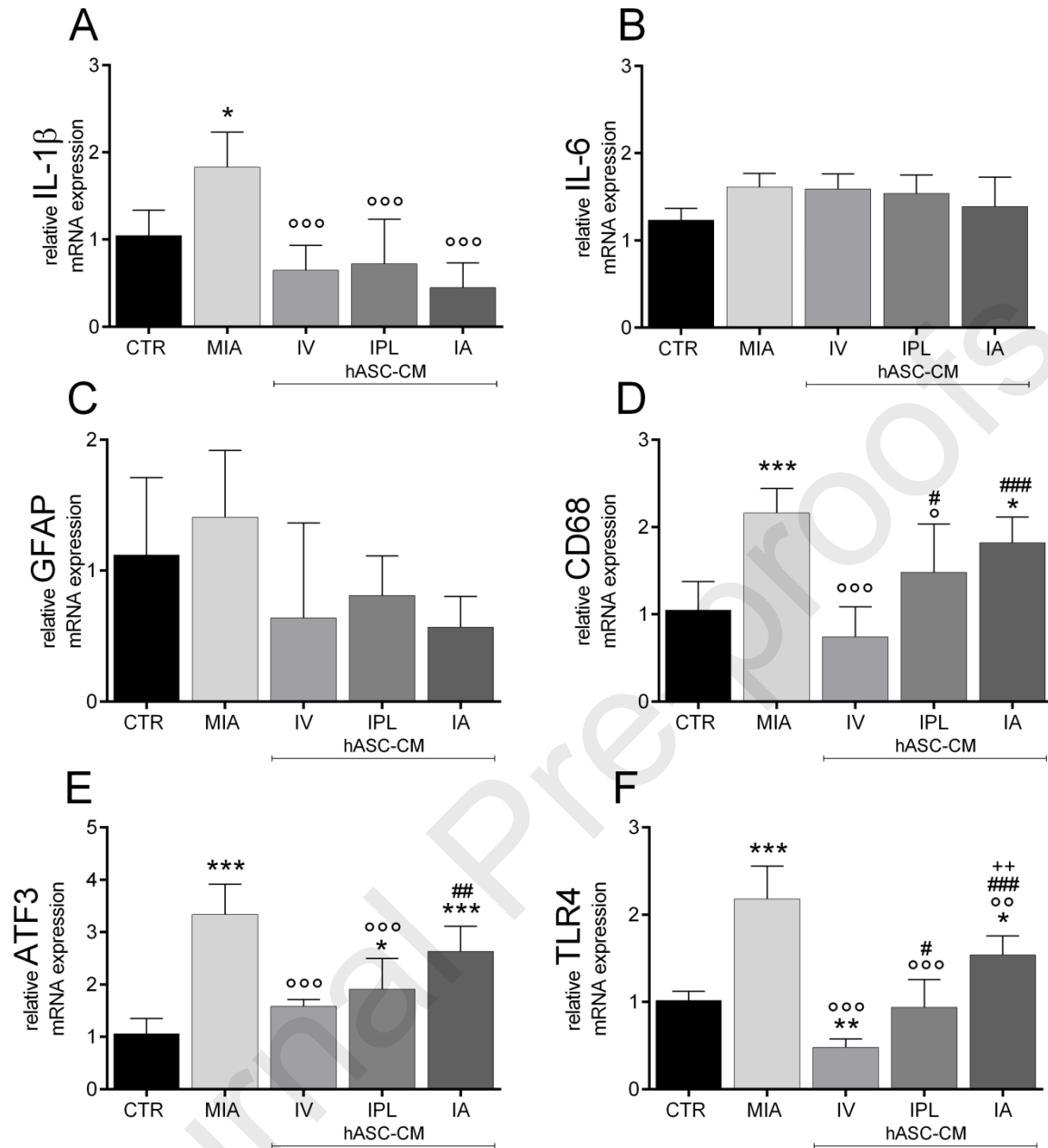
- Moschetti, G., Amodeo, G., Paladini, M.S., Molteni, R., Balboni, G., Panerai, A., Sacerdote, P., Franchi, S., 2019. Prokineticin 2 promotes and sustains neuroinflammation in vincristine treated mice: Focus on pain and emotional like behavior. *Brain Behav Immun.* 82:422-431. DOI: 10.1016/j.bbi.2019.09.012
- Muley, M., Krustev, E., Reid, A., McDougall, J., 2017. Prophylactic inhibition of neutrophil elastase prevents the development of chronic neuropathic pain in osteoarthritic mice. *J Neuroinflammation.* 14(1):168. DOI: 10.1186/s12974-017-0944-0.
- Niada, S., Giannasi, C., Ferreira, L.M., Milani, A., Arrigoni, E., Brini, A.T., 2016. 17 β -estradiol differently affects osteogenic differentiation of mesenchymal stem/stromal cells from adipose tissue and bone marrow. *Differentiation.* 92(5):291-297. DOI: 10.1016/j.diff.2016.04.001
- Niada, S., Giannasi, C., Gomarasca, M., Stanco, D., Casati, S., Brini, A.T., 2019. Adipose-derived stromal cell secretome reduces TNF α -induced hypertrophy and catabolic markers in primary human articular chondrocytes. *Stem Cell Res.* 38:101463. DOI: 10.1016/j.scr.2019.101463
- Niada, S., Giannasi, C., Gualerzi, A., Banfi, G., Brini, A.T., 2018. Differential proteomic analysis predicts appropriate applications for the secretome of adipose-derived mesenchymal stem/stromal cells and dermal fibroblasts. *Stem Cells Int.* 2018:7309031. DOI: 10.1155/2018/7309031
- Niada, S., Giannasi, C., Magagnotti, C., Andolfo, A. & Brini, A. T. 2020. Proteomic analysis of extracellular vesicles and conditioned medium from human adipose-derived stem/stromal cells and dermal fibroblasts. *J Proteomics*, 232, 104069.
- Noronha, N. C., Mizukami, A., Calíari-Oliveira, C., Cominal, J. G., Rocha, J. L. M., Covas, D. T., Swiech, K. & Malmegrim, K. C. R. 2019. Priming approaches to improve the efficacy of mesenchymal stromal cell-based therapies. *Stem Cell Res Ther*, 10, 131.
- Ogonna, C.A., Clark, A.K., Gentry, C., Hobbs, C., Malcangio, M., 2013. Pain-like behaviour and spinal changes in the monosodium iodoacetate model of osteoarthritis in C57Bl/6 mice. *Eur J Pain.* 17(4):514-526. DOI: 10.1002/j.1532-2149.2012.00223.x

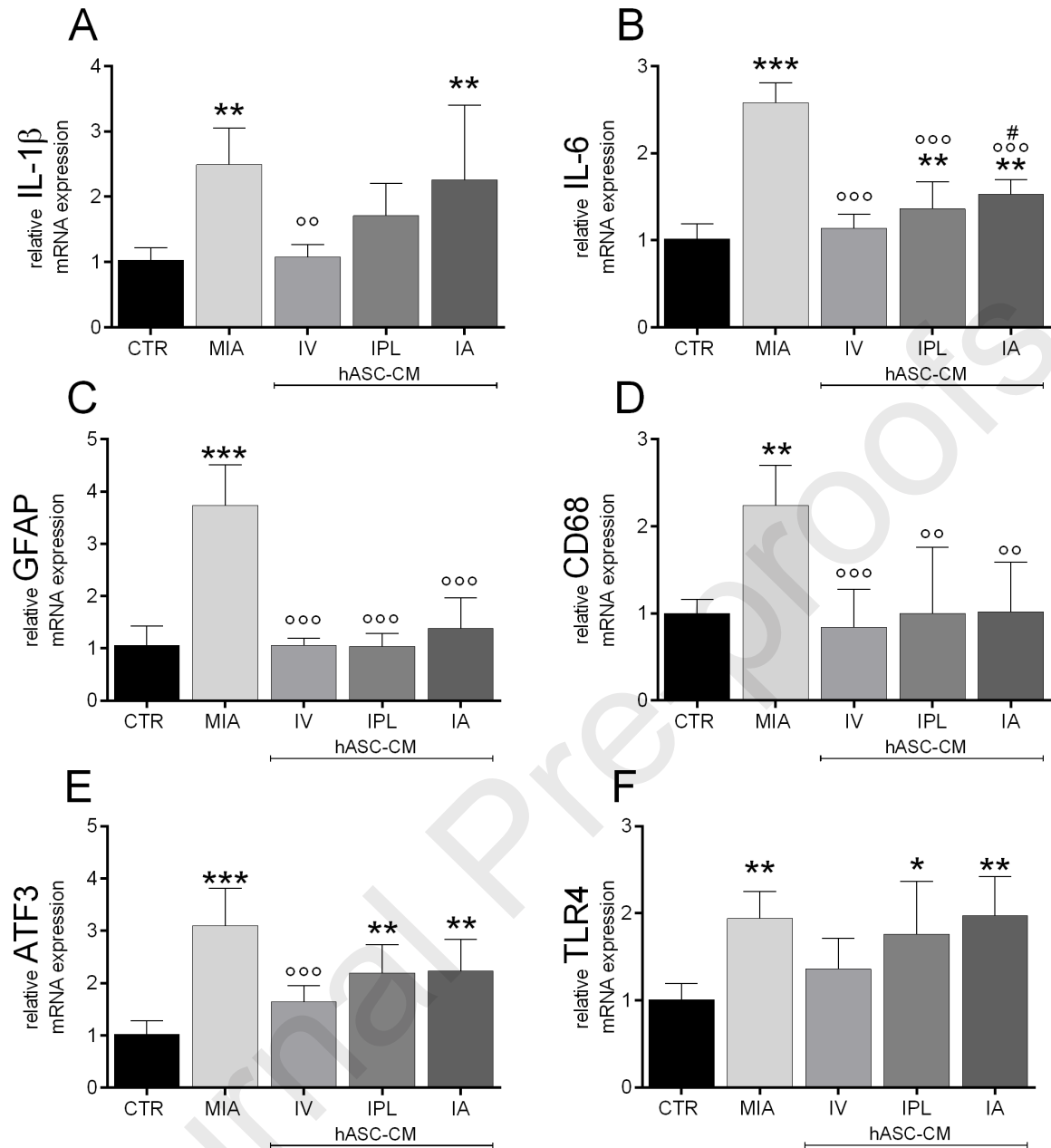
- Orita, S., Ishikawa, T., Miyagi, M., Ochiai, M., Inoue, G., Eguchi, Y., Kamoda, H., Arai, G., Toyone, T., Aoki, Y., Kubo, T., Takahashi, K., Ohtori, S., 2011. Pain-related sensory innervation in monoiodoacetate-induced osteoarthritis in rat knees that gradually develops neuronal injury in addition to inflammatory pain. *BMC Musculoskelet Disord.* 12:134. DOI: 10.1186/1471-2474-12-134
- Park, Y. B., Ha, C. W., Kim, J. A., Han, W. J., Rhim, J. H., Lee, H. J., Kim, K. J., Park, Y. G. & Chung, J. Y., 2017. Single-stage cell-based cartilage repair in a rabbit model: cell tracking and in vivo chondrogenesis of human umbilical cord blood-derived mesenchymal stem cells and hyaluronic acid hydrogel composite. *Osteoarthritis Cartilage*, 25, 570-580. DOI: 10.1016/j.joca.2016.10.012
- Praveen Kumar, L., Kandoi, S., Misra, R., Vijayalakshmi, S., Rajagopal, K., Verma, S.R., 2019. The mesenchymal stem cell secretome: A new paradigm towards cell-free therapeutic mode in regenerative medicine. *Cytokine Growth Factor Rev.* 46:1-9. (Review) DOI: 10.1016/j.cytogfr.2019.04.002
- Rainbow, R., Ren, W., Zeng, L., 2012. Inflammation and joint tissue interactions in OA: implications for potential therapeutic approaches. *Arthritis*. 2012:741582.
- Rajkovic, I., Wong, R., Lemarchand, E., Tinker, R., Allan, S.M., Pinteaux, E., 2019. Pentraxin 3 regulates neutrophil infiltration to the brain during neuroinflammation. *AMRC Open Res.* 1:10. DOI: 10.12688/amrcopenres.12875.1
- Satué, M., Schöler, C., Ginner, N., Erben, R. G., 2019. Intra-articularly injected mesenchymal stem cells promote cartilage regeneration, but do not permanently engraft in distant organs. *Sci Rep*, 9, 10153. DOI: 10.1038/s41598-019-46554-5
- Schaible, H.G., 2012. Mechanisms of chronic pain in osteoarthritis. *Curr Rheumatol Rep.* 14(6):549-556. (Review) DOI: 10.1007/s11926-012-0279-x
- Steinert, A.F., Rackwitz, L., Gilbert, F., Nöth, U., Tuan, R.S., 2012. Concise review: the clinical application of mesenchymal stem cells for musculoskeletal regeneration: current status and perspectives. *Stem Cells Transl Med.* 1(3):237-247. (Review) DOI: 10.5966/sctm.2011-0036

- Suokas, A.K., Walsh, D.A., McWilliams, D.F., Condon, L., Moreton, B., Wylde, V., Arendt-Nielsen, L., Zhang, W., 2012. Quantitative sensory testing in painful osteoarthritis: a systematic review and meta-analysis. *Osteoarthritis Cartilage*. 20(10):1075-1085. (Review) DOI: 10.1016/j.joca.2012.06.009
- Szklarczyk, D., Franceschini, A., Wyder, S., Forslund, K., Heller, D., Huerta-Cepas, J., Simonovic, M., Roth, A., Santos, A., Tsafou, K.P., Kuhn, M., Bork, P., Jensen, L.J., von Mering, C., 2015. STRING v10: protein-protein interaction networks, integrated over the tree of life. *Nucleic Acids Res.* 43(Database issue):D447-452. DOI: 10.1093/nar/gku1003
- Thakur, M., Rahman, W., Hobbs, C., Dickenson, A.H., Bennett, D.L.H., 2012. Characterisation of a peripheral neuropathic component of the rat monoiodoacetate model of osteoarthritis. *PLoS One* 7(3):e33730. DOI: 10.1371/journal.pone.0033730
- Volarevic, V., Markovic, B.S., Gazdic, M., Volarevic, A., Jovicic, N., Arsenijevic, N., Armstrong, L., Djonov, V., Lako, M., Stojkovic, M., 2018. Ethical and Safety Issues of Stem Cell-Based Therapy. *Int J Med Sci.* 15(1):36-45. DOI: 10.7150/ijms.21666.
- Yiou, R., Mahrouf-Yorgov, M., Trébeau, C., Zanaty, M., Lecointe, C., Souktani, R., Zadigue, P., Figeac, F., Rodriguez, A.M., 2016. Delivery of human mesenchymal adipose-derived stem cells restores multiple urological dysfunctions in a rat model mimicking radical prostatectomy damages through tissue-specific paracrine mechanisms. *Stem Cells*.34:392–404. DOI: 10.1002/stem.2226
- Zhang, R-X., Ren, K., Dubner, R., 2013. Osteoarthritis pain mechanisms: basic studies in animal models. *Osteoarthritis Cartilage*. 21(9):1308-1315. (Review) DOI: 10.1016/j.joca.2013.06.013
- Zhu, X., Li, X., Zhu, M., Xu, K., Yang, L., Han, B., Huang, R., Zhang, A., Yao, H., 2018. Metalloprotease Adam10 suppresses epilepsy through repression of hippocampal neuroinflammation. *J Neuroinflammation* 15(1):221. DOI: 10.1186/s12974-018-1260-z





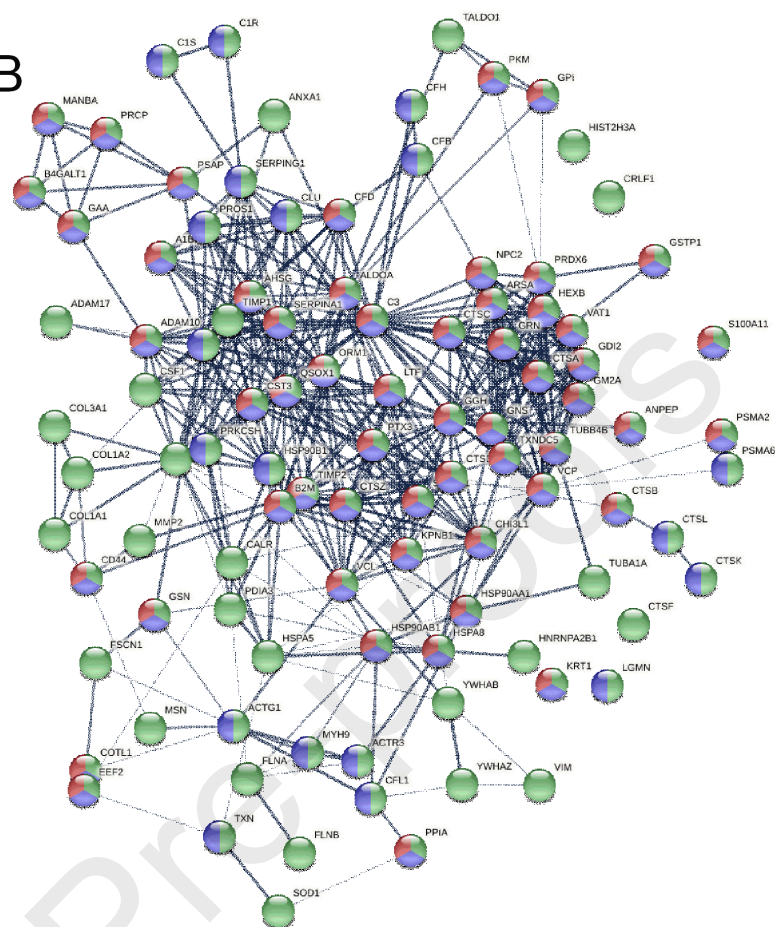




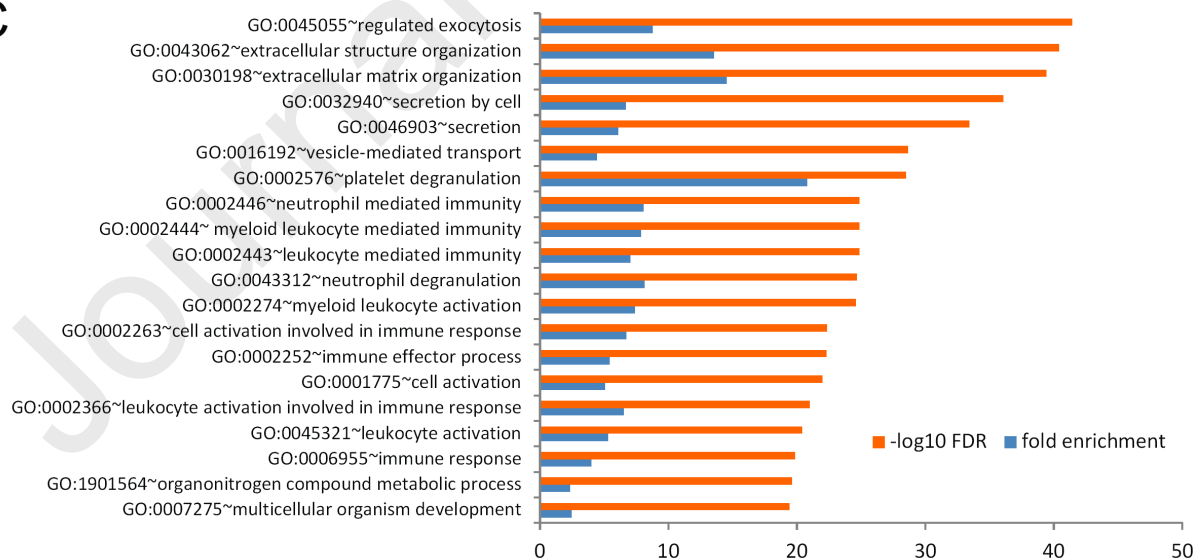
A

Reactome Pathways		
<i>#term ID and Description</i>	<i>Count in gene set</i>	<i>FDR</i>
HSA-1474244~Extracellular matrix organization	70 of 298	2.6e-50
HSA-114608~Platelet degranulation	42 of 125	1.1e-34
HSA-381426~Regulation of IGF transport and ...	40 of 123	9.13e-33
HSA-8957275~Post-translational protein phosphorylation	38 of 106	1.8e-32
HSA-76002~Platelet activation, signaling and aggregation	45 of 256	2.9e-27
HSA-6798695~Neutrophil degranulation	56 of 471	1.5e-26
HSA-1474228~Degradation of the extracellular matrix	34 of 139	1.8e-24
HSA-168249~Innate Immune System	75 of 1012	4.8e-24
HSA-3000178~ECM proteoglycans	27 of 75	4.8e-23
HSA-168256~Immune System	101 of 1925	2.4e-22

B



C



- Pain and neuroinflammation in nerve, DRG and spinal cord are present in osteoarthritic mice

- Human adipose-derived mesenchymal stem cell secretome induces fast and lasting relief of hypersensitivity
- Reduction with secretome of neuroinflammation in nerve, dorsal root ganglia and spinal cord
- The IV route is more efficacious than the intra-plantar or intra-articular ones on pain and neuroinflammation
- The effect of secretome is exerted in the nervous system rather than in the joint.